Expanded View Figures

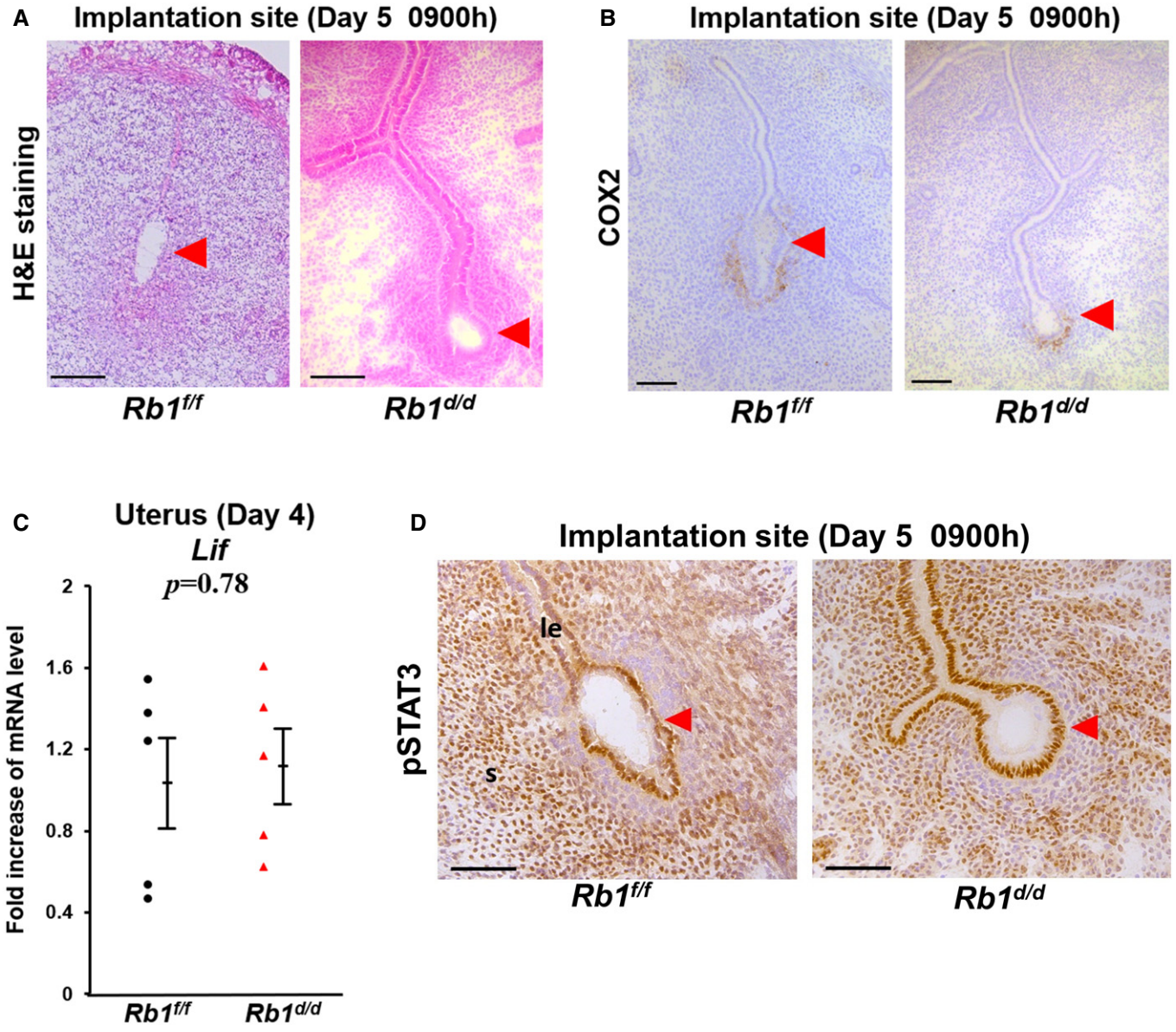

Figure EV1. Embryo attachment occurs normally in *Rb1*$^{d/d}$ mice.

A H&E staining of implantation sites in *Rb1*$^{f/f}$ and *Rb1*$^{d/d}$ mice at 09:00 h on day 5 of pregnancy. Scale bar = 100 μm; arrowhead, embryo.

B Immunostaining of COX2, a marker of embryo attachment reaction in the implantation sites of *Rb1*$^{f/f}$ and *Rb1*$^{d/d}$ mice at 09:00 h on day 5 of pregnancy. Scale bar = 100 μm; arrowhead, embryo.

C Uterine expression of *Lif* mRNA on day 4 of pregnancy was comparable between *Rb1*$^{f/f}$ and *Rb1*$^{d/d}$ mice (mean ± SEM, Student's *t*-test; n = 5 mice for each group).

D Immunostaining of pSTAT3, a marker of activated LIF signaling in the implantation sites of *Rb1*$^{f/f}$ and *Rb1*$^{d/d}$ mice at 09:00 h on day 5 of pregnancy. Scale bar = 100 μm; le, luminal epithelium; s, stroma; arrowhead, embryo.

Data information: le, luminal epithelium; s, stroma

© 2021 The Authors

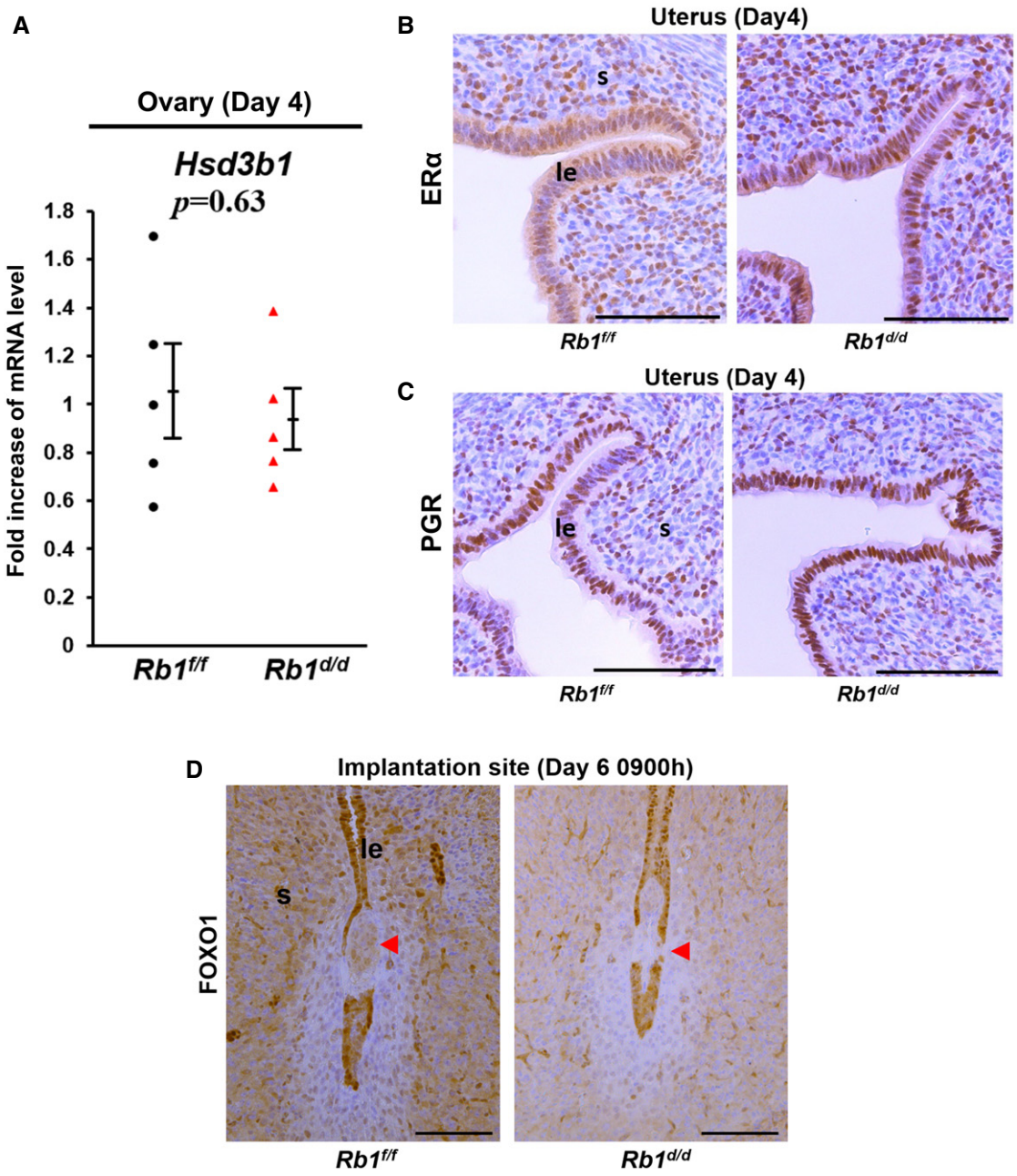

Figure EV2. Normal expressions of ovarian *Hsd3b1* mRNA and uterine estrogen receptor α (ERα), progesterone receptor (PGR), and FOXO1 proteins in $Rb1^{d/d}$ mice.

A Quantitative PCR demonstrated that ovarian expression of ovarian steroidogenic enzyme *Hsd3b1* mRNA was comparable between $Rb1^{f/f}$ and $Rb1^{d/d}$ mice on day 4 of pregnancy (mean ± SEM, Student's *t*-test; $n = 5$ mice for each group).

B, C Immunohistochemistry demonstrated that uterine expression of ERα and PGR was comparable between $Rb1^{f/f}$ and $Rb1^{d/d}$ mice on day 4 of pregnancy. Scale bar = 100 μm.

D Immunohistochemistry demonstrated that uterine expression of FOXO1 was comparable between $Rb1^{f/f}$ and $Rb1^{d/d}$ mice on day 6 of pregnancy. Scale bar = 100 μm; arrowhead, embryo.

Data information: le, luminal epithelium; s, stroma.

© 2021 The Authors

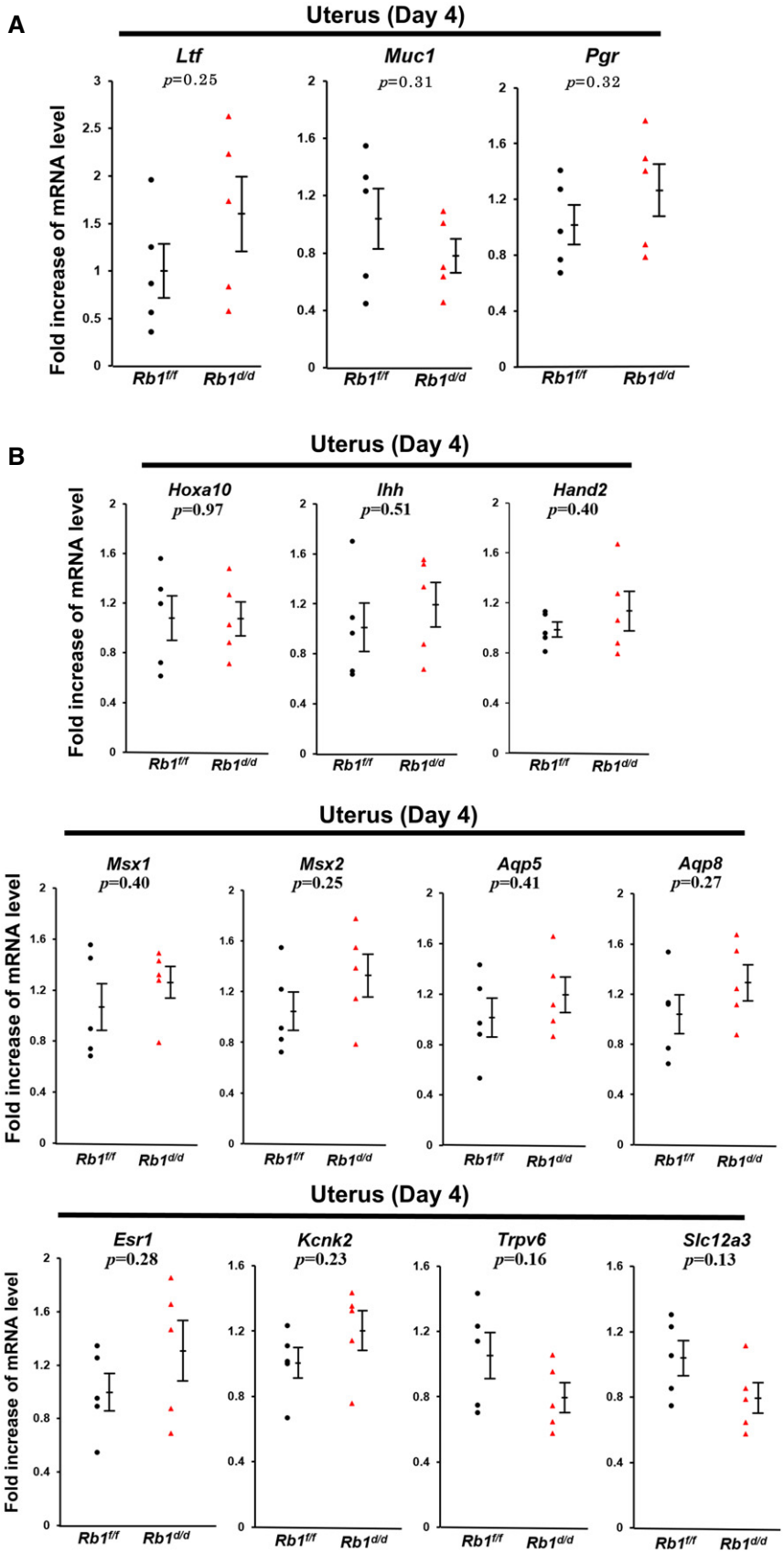

Figure EV3. Comparable uterine expressions of E_2-responsive and P_4-responsive genes in *Rb1*$^{f/f}$ and *Rb1*$^{d/d}$ mice on day 4 of pregnancy.

A, B Quantitative PCR demonstrated that uterine expression of E_2-responsive (A) and P_4-responsive genes (B) was comparable between *Rb1*$^{f/f}$ and *Rb1*$^{d/d}$ mice on day 4 of pregnancy (mean ± SEM, Student's *t*-test; $n = 5$ mice for each group).

© 2021 The Authors

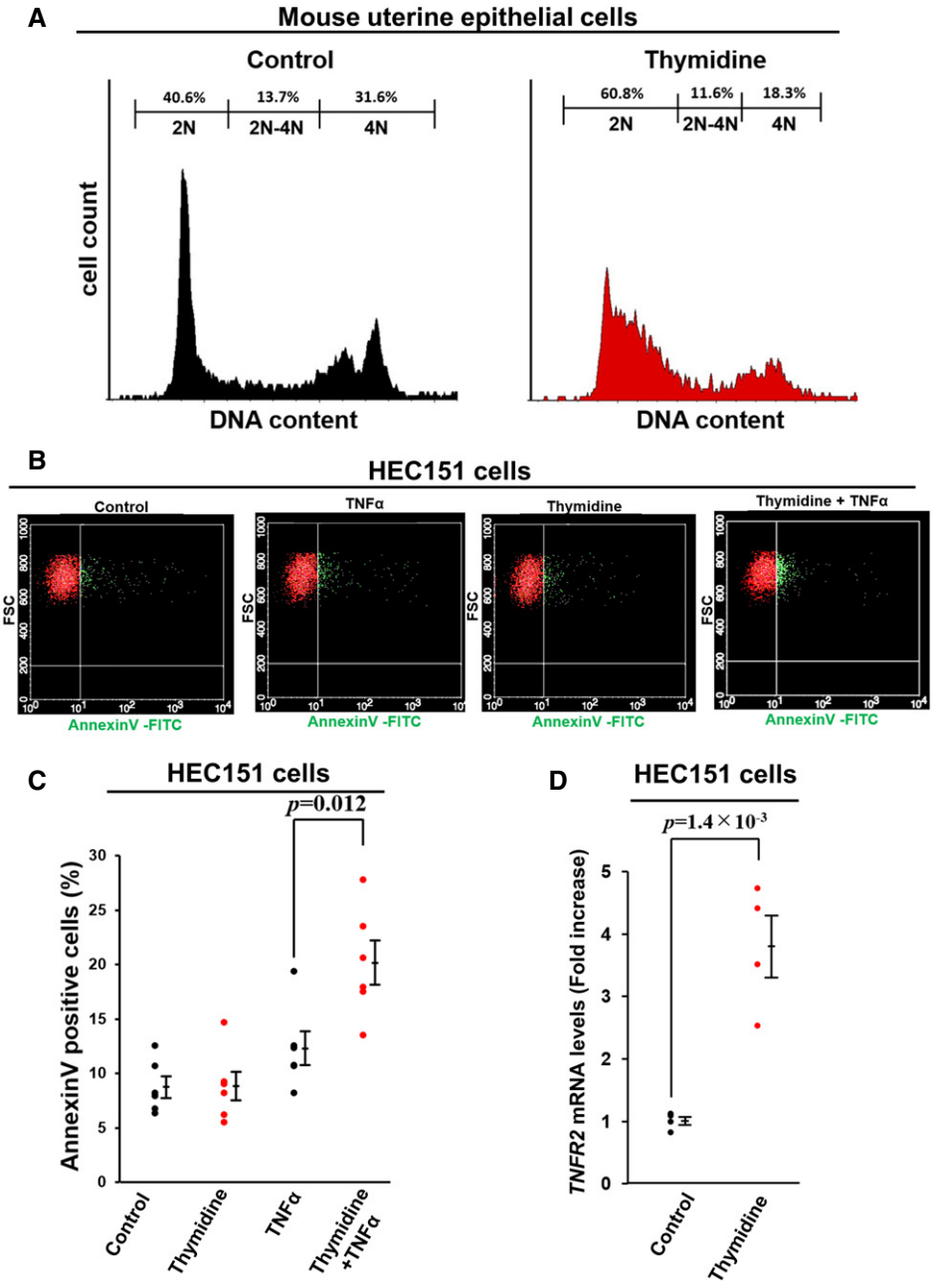

Figure EV4. Thymidine-induced cell cycle arrest in primary mouse epithelial cells and HEC151 endometrial epithelial cell line.

A Thymidine-induced cell cycle arrest in primary mouse epithelial cells. Mouse uterine epithelial cells were stained with propidium iodine, and cell fractions were quantified by flow cytometry.

B, C Annexin V assay using a human endometrial epithelial cell line HEC151 showed that TNFα administration increases the expression of annexin V in growth-arrested HEC151 cells with thymidine treatment, but does not in the control cells (mean ± SEM, Student's *t*-test). The assay was performed in duplicate for each group, and the examination was performed three times.

D The expression of TNF receptor type 2 (TNFR2) was upregulated in growth-arrested HEC151 cells with thymidine treatment (mean ± SEM, Student's *t*-test). Quantitative PCR was performed in quadruplicate for each group.

© 2021 The Authors

Figure EV5. RNA-seq analyses using uterine epithelium of *Rb1*$^{f/f}$ and *Rb1*$^{d/d}$ mice on day 4 of pregnancy.

A Day 4 uteri were collected from *Rb1*$^{f/f}$, *Rb1*$^{d/d}$, P_4-primed *Rb1*$^{f/f}$, and P_4-primed *Rb1*$^{d/d}$ mice. As for P_4-primed *Rb1*$^{f/f}$ and *Rb1*$^{d/d}$ mice, pre-implantation P_4 treatment (2 mg/mouse/day) was performed on days 2 and 3 of pregnancy. RNA-seq was performed using the uterine luminal epithelium dissected out by laser capture microdissection. The heatmaps depicted $\log_2$ fold enrichment of differentially expressed genes (DEGs) among the uterine epithelium. Clusters were defined by k-means clustering. Each DEG has a $\log_2$ fold change > |1| in at least one group comparing to others. Numbers shown in right indicate different gene clusters and numbers of DEGs in each cluster.

B Gene regulatory systems in the gene cluster 6 in which the transcripts are poorly expressed in *Rb1*$^{d/d}$ mice without P_4 supplementation compared with other groups were predicted in Enrichr by comparing our data with publicly available datasets as for transcriptional factors. DEGs in the cluster 6 were highly correlated with cell cycle-related TFs such as serum response factor (SRF) and E2F8.

C GO terms analyses by Enrichr for the cluster 6 demonstrated that the genes related to epithelial differentiation and inhibition of cell proliferation are downregulated in the luminal epithelium of *Rb1*$^{d/d}$ mice without P_4 treatment.

D The heatmap of cell cycle-related genes in the luminal epithelium of *Rb1*$^{f/f}$ and *Rb1*$^{d/d}$ mice with and without pre-implantation P_4 treatment was demonstrated. Cyclin-dependent kinase inhibitors CDKN2A (p21) and CDKN2C (p18) were upregulated in *Rb1*$^{f/f}$ and *Rb1*$^{d/d}$ mice with P_4 treatment compared with *Rb1*$^{d/d}$ mice without P_4 treatment. Yellow, blue, and black indicate high, intermediate, and low gene expression, respectively.

E Immunohistochemistry of CDKN2C (p18) protein in the uterus of *Rb1*$^{f/f}$ and *Rb1*$^{d/d}$ mice with and without P_4 treatment. Same as transcriptome analysis, CDKN2C staining was intense in the uteri of *Rb1*$^{f/f}$ and *Rb1*$^{d/d}$ mice with P_4 treatment compared with *Rb1*$^{d/d}$ mice without P_4 treatment. Scale bar = 100 μm; le, luminal epithelium; s, stroma.

© 2021 The Authors

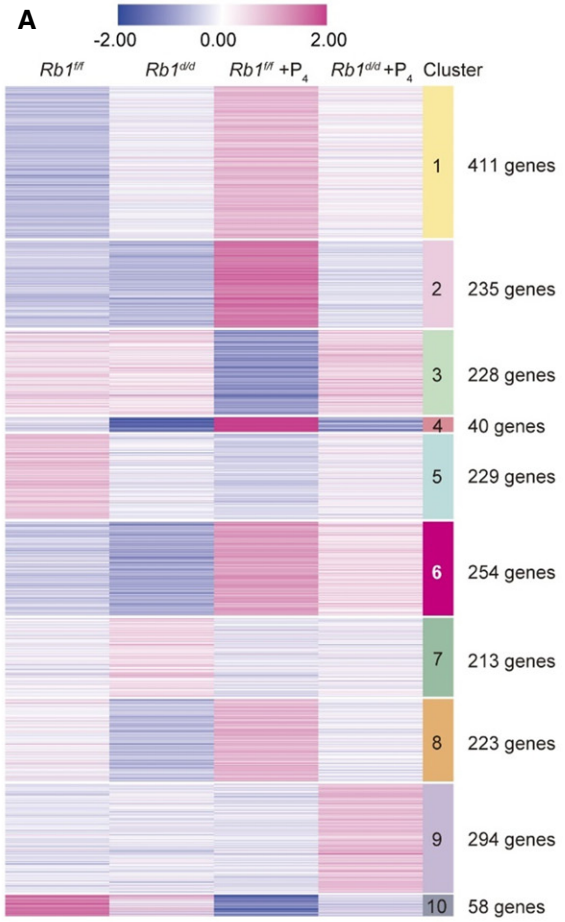

B

Comparison analyses with published data regarding transcriptional factors

	P values
SRF KO MOUSE GSE34545 CREEDSID GENE 2884 UP	8.02×10^{-18}
MYCN OE MOUSE GSE6077 CREEDSID GENE 40 DOWN	4.17×10^{-15}
ZFX KO MOUSE GSE7069 CREEDSID GENE 177 UP	1.92×10^{-14}
POU5F1 KD HUMAN GSE21135 CREEDSID GENE 1328 UP	2.58×10^{-13}
NEUROD1 KO MOUSE GSE35396 CREEDSID GENE 3091 DOWN	3.74×10^{-13}
POU5F1 KD HUMAN GSE21135 CREEDSID GENE 1329 UP	1.55×10^{-10}
HEY2 KO MOUSE GSE6526 CREEDSID GENE 1508 DOWN	1.82×10^{-10}
HEY2 KO MOUSE GSE6526 CREEDSID GENE 1509 UP	2.11×10^{-10}
E2F8 KO MOUSE GSE52157 CREEDSID GENE 2828 DOWN	4.64×10^{-10}
RUNX1 KO MOUSE GSE34292 CREEDSID GENE 2397 UP	6.11×10^{-10}

C

GO analyses

	P values
positive regulation of cell differentiation (GO:0045597)	1.98×10^{-7}
positive regulation of epithelial to mesenchymal transition (GO:0010718)	6.40×10^{-7}
negative regulation of cellular process (GO:0048523)	5.08×10^{-6}
regulation of pathway-restricted SMAD protein phosphorylation (GO:0060393)	9.53×10^{-6}
positive regulation of pathway-restricted SMAD protein phosphorylation (GO:0010862)	2.75×10^{-5}
leukocyte aggregation (GO:0070486)	6.82×10^{-5}
positive regulation of transmembrane receptor protein serine/threonine kinase signaling pathway (GO:0090100)	8.29×10^{-5}
positive regulation of epithelial cell differentiation (GO:0030858)	8.47×10^{-5}
negative regulation of mitotic nuclear division (GO:0045839)	1.61×10^{-4}
branching morphogenesis of an epithelial tube (GO:0048754)	2.06×10^{-4}

D

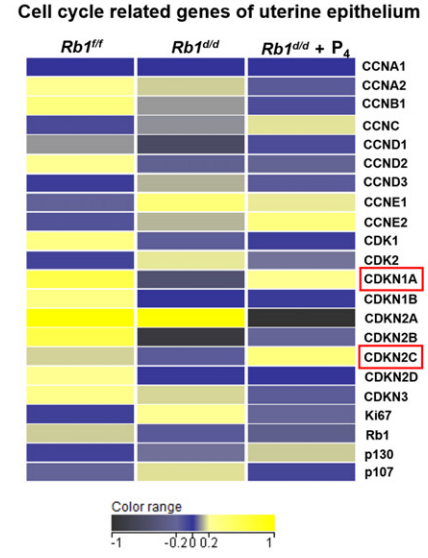

E

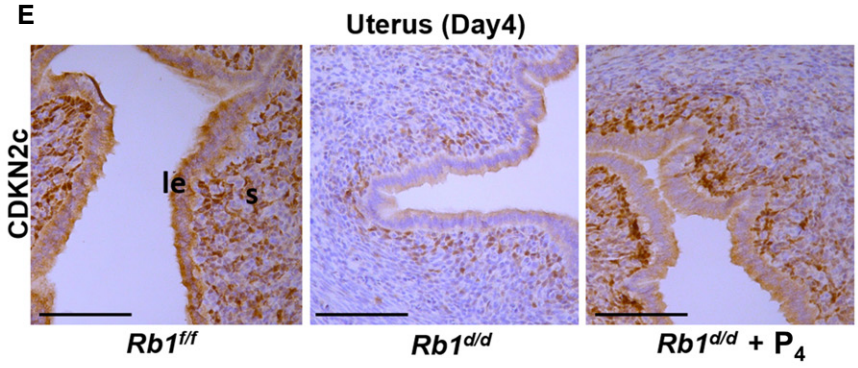

Figure EV5.

© 2021 The Authors